The synthesis of single-walled carbon nanotubes with controlled length and bundle size using the electric arc method

Feng Du, Yanfeng Ma, Xin Lv, Yi Huang, Feifei Li, Yongsheng Chen *

Center for Nanoscale Science and Technology & Key Laboratory for Functional Polymer Materials, Institute of Polymer Chemistry, Nankai University, Tianjin 300071, China

Great strides have been made for the synthesis of single-walled carbon nanotubes (SWNTs) over the past decade [1–3]. Among the three major techniques, the electrical arc (EA) method is believed to be one of the most efficient techniques for large-scale synthesis of the as-prepared (AP) SWNT product [4]. While the chemical vapor deposition (CVD) method has the advantage of controlled growth [5,6], as far as we are aware that there is no report to control the growth of SWNTs using the EA method. Also the AP-SWNTs produced using each of these techniques always come with various impurities including primarily amorphous carbon, metal catalysts [7]. In this letter, we report a simple EA approach, in which high quality SWNTs at large-scale can be obtained with its length and bundle size controlled.

Motivated by the recent work by Iijima et al. [3], we intended to find an oxidizer that would preferably remove amorphous carbon at the growth temperature for the EA method. We found that not only CO_2 acts well for this purpose, more importantly we can also produce SWNTs in different lengths and bundle sizes by varying its concentration in the buffer gas. The products were evaluated using Raman spectroscopy, thermogravimetric analysis (TGA), scanning electron microscopy (SEM), transmission electron microscopy (TEM) and atom force microscopy (AFM).

The EA apparatus and experimental conditions were similar to the literature described earlier [8]. The electrodes were 20 mm in diameter and 200–250 mm in length. All of the EA experiments were carried out under a He buffer gas with 0–20 volume (v)% CO_2 in it at a total pressure of 530–550 Torr. Typical run time was 70 min, leading to the production of 20–30 g of AP-SWNT soot per anode. The yield of the AP-SWNT product, defined as the ratio of the weight of web and chamber fractions to the total weight of material collected, was in the range of 45–50%.

Comparing the nanotubes we got with that from using pure He buffer [4,8], several different features were observed. The first is that the SWNT bundles became shorter and smaller as seen from the TEM images. AFM was further used to do a statistics analysis for a quantitative conclusion. Figs. 1 and 2 show the AFM results for the SWNT length and its bundle size for the typical SWNT soot products under the 0, 5 and 10 v% CO_2/He conditions and we can see a clear trend that both the SWNT length and its bundle size decrease with more CO_2 used. For example, compared with that prepared under pure He buffer, the average length of SWNT bundles decreased from 1.43 μm to 0.74 μm for the 10 v% condition. A similar trend was found for the bundle diameters.

Fig. 3 shows the results of TGA from the AP SWNTs with different ratios of CO_2/He. The dotted line (DSC) shows two peaks ~340 °C and 410 °C. The first peak is usually associated with amorphous carbon and the second with SWNTs [4]. While it is difficult to get an accurate estimation of the three major components due to the heterogeneous nature of the SWNTs products [4], the TGA shows that the SWNTs from this process yields similar amount of metal oxide residue (~33%). With the increasing ratio of CO_2/He, the first peak of the DSC decreases significantly, indicating that the SWNT products have less amorphous carbon with the increase of CO_2 concentration. While the yield hardly changes with the concentration of CO_2 up to 10 v%, the overall yield of SWNTs starts to drop significantly when CO_2 is over 10 v%. We also found that the metal catalyst used for the synthesis is much easier to be removed. After a simple acid purification, TGA (Fig. 4) shows most of the metal impurity to be removed and the carbonaceous materials to be up to 94 wt% compared with 87 wt% for the SWNT soot from the He condition.

Less amorphous carbon on the SWNTs generated using CO_2 is also confirmed with the TEM studies. Fig. 5 shows

---

* Corresponding author. Tel.: +86 22 2350 0693; fax: +86 22 2350 2749.
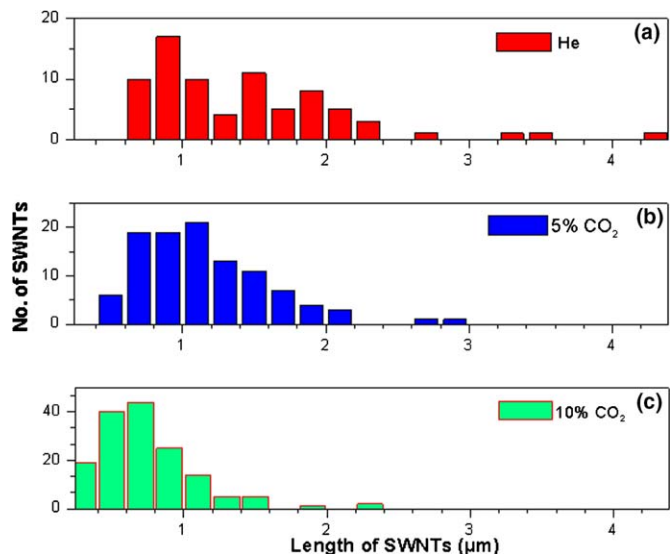
E-mail address: yschen99@nankai.edu.cn (Y. Chen).

Fig. 1. AFM length analysis of SWNTs. SWNTs prepared under: (a) pure He buffer gas, (b) 5 v% CO_2/He buffer gas and (c) under 10 v% CO_2/He buffer gas. The average length of SWNTs are 1.43, 1.15, and 0.74 µm for 0%, 5% and 10% CO_2/He buffer gas, respectively. Error was estimated to be ~8%. All samples (1 mg) were prepared in DMF (100 ml) using sonication for 2 h for the subsequent AFM characterization.

Fig. 2. AFM bundle diameter analysis of SWNTs. SWNTs prepared under: (a) pure He buffer gas, (b) 5 v% CO_2/He buffer gas and (c) under 10 v% CO_2/He buffer gas. The average diameters of SWNTs are 5.95, 5.00, and 5.32 nm for 0%, 5% and 10% CO_2/He buffer gas, respectively. Error was estimated to be ~8%.

the typical lower and high resolution TEM images for the SWNT soot generated under the He and 10 v% CO_2 conditions. It can be seen clearly that the product from pure He had more amorphous carbon on the surface of SWNT bundles and the surface of SWNTs from CO_2 condition is much smoother.
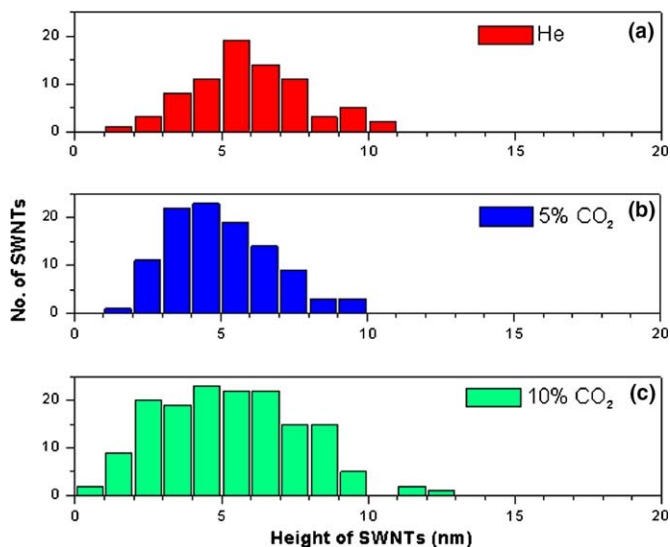
It is believed that two of the key issues for the optimization of SWNT growth are the metal catalyst particle size and its existence time. And the oversize of these particles due to overcoating of amorphous carbon would favor other no-tubular (impurity) structure formation [3,9]. Considering the lower resistance of amorphous carbon to oxidation than that of SWNTs, we believe the Boudouard
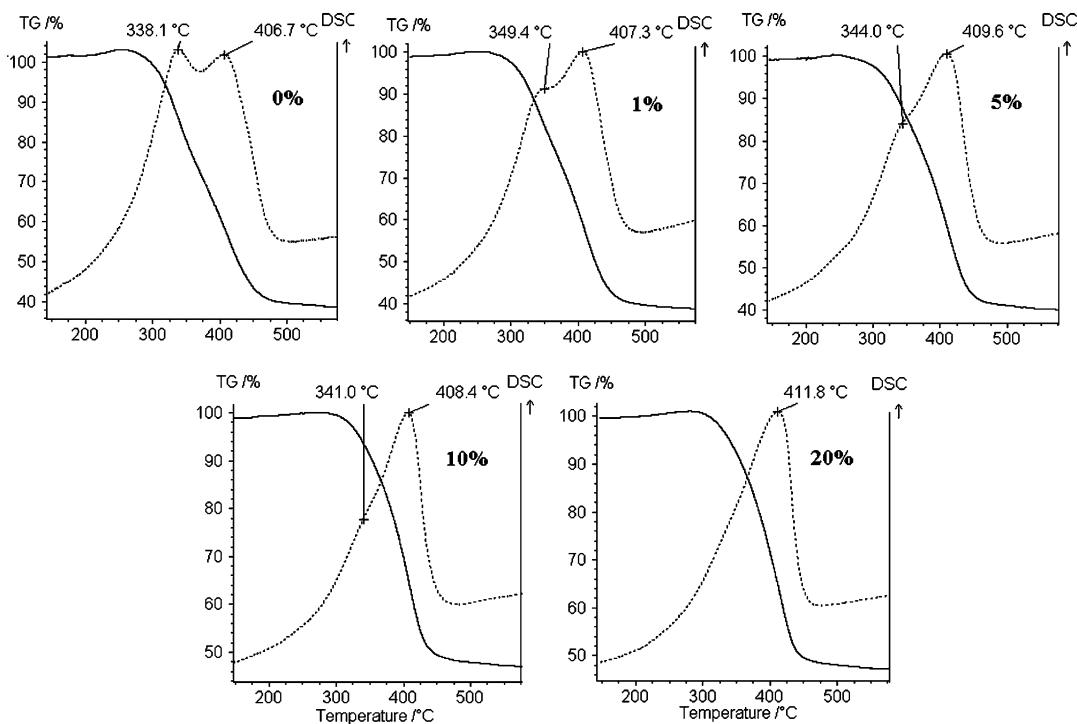

Fig. 3. TGA analysis in a mixture of 20% O_2 and 80% N_2 (25 mln/min total volume flow) showing weight (black lines) and DSC (dotted lines) with respect to temperature for the soot part of the AP-SWNT soot prepared with varying CO_2 concentration in a He atmosphere. Heating rate 2 K/min.
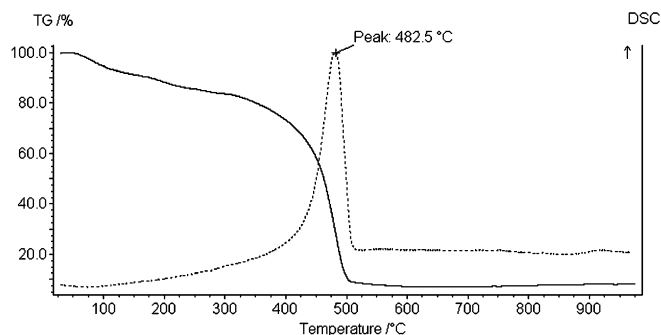
Fig. 4. TGA analysis in a mixture of 20% O_2 and 80% N_2 (25 mln/min total volume flow) and DSC (dotted lines) with respect to temperature for the purified SWNTs (refluxing in 2.6 M HNO_3 for 12 h and drying under vacuum for 10 h). The SWNT soot was obtained under 10 v% carbon dioxide. The metal oxide residue was ~6.0 wt%.

reaction ($CO_2 + C \rightarrow 2CO$) likely occurring in the vicinity area of the EA acing might be the reason to reduce the amorphous carbon overcoating on SWNTs and the metal particles [3,9]. So it is reasonable to argue that CO_2 would burn away the amorphous carbon overcoating on the "poised" metal catalyst nanoparticles, which would increase the catalyst lifetime and also make the subsequent purification steps easier.

The SWNTs were also characterized with Raman spectra (not shown) and they show similar features for different CO_2 concentrations. Using the radical breathing mode frequency [10], the diameter of SWNTs were estimated to be in the range of 1.2–1.8 nm, comparable to that of the SWNTs using He and in consistent with the result from TEM (Fig. 5). The similar size of the SWNT diameters suggests that the nucleation step of SWNTs growth, which is believed to control the SWNT diameters [3,9], is not affected by the addition of CO_2 under our conditions.

The exact mechanism is not clear why we got smaller and shorter bundles of SWNTs using the He/CO_2 condition. Two possibilities are: the SWNT bundles are grown shorter (disruption of the growing or more growing sites) or the SWNTs are oxidized into smaller ones by CO_2, similar to the acid-oxidation or other similar methods used widely in the literatures for cutting SWNTs. Further investigation is underway for this issue.

In summary, our CO_2 assisted EA approach is able to produce SWNTs with controlled length and bundle size and much less amorphous carbon. The SWNT bundles are smaller and shorter and the metal impurity is readily to be removed. Combining with the overall ease and low cost advantages of the EA method, these results present a potential opportunity for the controllable and large-scale production of SWNTs.
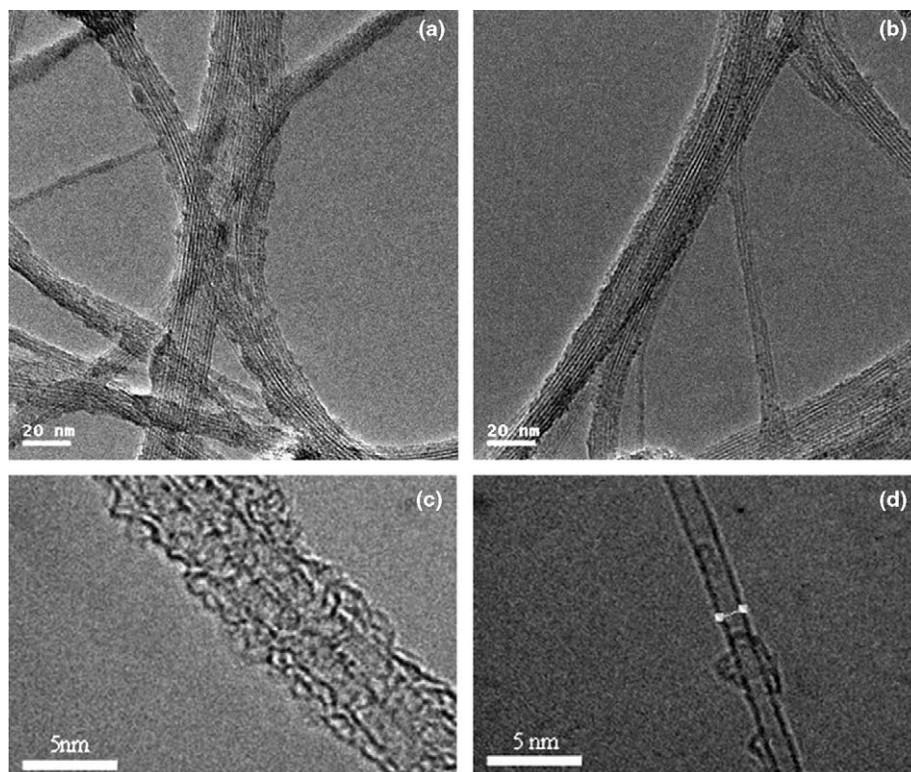

Fig. 5. The lower and high magnification TEM images of AP SWNTs: the lower magnification TEM images using He (a) and 10 v% CO_2/He (b) buffer gas; the higher magnification TEM images of a SWNT bundle with two SWNTs and an individual SWNT using pure He (c) and 10 v% CO_2/He (d) buffer gas.

Acknowledgments

References

[1] Liu C, Cheng HM, Cong HT, Li F, Su G, Zhou BL, et al. Synthesis of macroscopically long ropes of well-aligned single-walled carbon nanotubes. Adv Mater 2000;12(16):1190–2.

[2] Nikolaev P, Bronikowski M, Bradley RK, Rohmund F, Colbert DT, Smith KA, et al. Gas-phase catalytic growth of single-walled carbon nanotubes from carbon monooxide. Chem Phys Lett 1999;313(1–2):91–7.

[3] Hata K, Futaba DN, Mizuno K, Namai T, Yumura M, Iijima S. Water-assisted highly efficient synthesis of impurity-free single-walled carbon nanotubes. Science 2004;306(5700):1362–4.

[4] Itkis ME, Perea DE, Niyogi S, Love J, Tang J, Yu A, et al. Optimization of the Ni–Y catalyst composition in bulk electric arc synthesis of single-walled carbon nanotubes by use of near-infrared spectroscopy. J Phys Chem B 2004;108(34):12770–5.

[5] Kong J, Soh HT, Cassell AM, Quate CF, Dai HJ. Synthesis of individual single-walled carbon nanotubes on patterned silicon wafers. Nature 1998;395(6705):878–81.

[6] Cheung CL, Kurtz A, Park H, Lieber CM. Diameter-controlled synthesis of carbon nanotubes. J Phys Chem B 2002;106(10):2429–33.

[7] Landi BJ, Ruf HJ, Evans CM, Cress CD, Raffaelle RP. Purity assessment of single-wall carbon nanotubes, using optical absorption spectroscopy. J Phys Chem B 2005;109(20):9952–65.

[8] Lv X, Du F, Ma YF, Wu Q, Chen YS. Synthesis of high quality single-walled carbon nanotubes at large scale by electric arc using metal compounds. Carbon 2005;43(9):2020–2.

[9] Gorbunov A, Jost O, Pompe W, Graff A. Solid-liquid-solid growth mechanism of single-wall carbon nanotubes. Carbon 2002;40(1):113–8.

[10] Rao AM, Chen J, Richter E, Schlecht U, Eklund PC, Haddon RC, et al. Effect of van der Waals interactions on the raman modes in single walled carbon nanotubes. Phys Rev Lett 2001;86(17):3895–8.

The effect of cooling rate on hydrogen release from a pyrolytic carbon coating and its resulting morphology

Boris Reznik [a,*], Koyo Norinaga [b], Dagmar Gerthsen [a], Olaf Deutschmann [b]

[a] *Laboratory for Electron Microscopy, University of Karlsruhe, 76128 Karlsruhe, Germany*
[b] *Institute for Chemical Technology and Polymer Chemistry, University of Karlsruhe, 76128 Karlsruhe, Germany*

The formation mechanism of deposits of pyrolytic carbon is a complex process involving homogeneous reactions in the gas phase, heterogeneous reactions at the substrate surface and subsequent dehydrogenation. All three processes are relevant for the final carbon structure and other physical properties [1,2]. Many studies are devoted to the analysis of the products of the hydrocarbon pyrolysis [1–4]. However, up to now experimental results demonstrating directly the dehydrogenation process have not yet been presented. Presumably the dehydrogenation process can be controlled by the thermal treatment of the deposit after the termination of the deposition, e.g. by the reactor cooling rate. In the present work, we study the effect of cooling rate on the release of hydrogen from a pyrolytic carbon coating and its resulting morphology.

Pyrolytic carbon coatings were deposited onto monolithic cordierite substrates placed in a vertical flow hot wall reactor by using ethene with a purity of better than 99.4% as the hydrocarbon precursor. The hot wall reactor used in this study is identical with the reactor described in a previous study [5]. Briefly, the deposition space is formed by a cylindrically shaped alumina tube with a diameter of 22 mm and a length of 40 mm. The inlet and outlet tubes of the reactor (8 mm in diameter) are connected to the deposition space through conical inlet and outlet nozzles. A channel structure, made of cordierite, with 25 channels per square inch, i.e. 4.4×4.4 mm^2/channel, is fitted in the alumina tube, resulting in a surface area/volume ratio of the deposition space of $[A/V] = 0.9$ mm^{-1}. The deposition experiments were performed at 950 °C, 4 kPa ethene pressure, and a residence time of 1 s. After a deposition duration of 70 h, the supply of ethene was stopped and argon was supplied with a flow rate of 33 ml/min. The reactor was then cooled down to room temperature. To reveal